Resistance switching of Au-implanted-ZrO_2 film for nonvolatile memory application

Qi Liu,[1,2] Weihua Guan,[1] Shibing Long,[1] Ming Liu,[1,a)] Sen Zhang,[1] Qin Wang,[1] and Junning Chen[2]
[1]*Laboratory of Nano-Fabrication and Novel Devices Integrated Technology, Institute of Microelectronics, Chinese Academy of Sciences, Beijing 100029, China*
[2]*College of Electronics and Technology, Anhui University, Hefei 230039, China*

(Received 1 July 2008; accepted 17 October 2008; published online 9 December 2008)

The resistive switching characteristics and switching mechanisms of the Au-implanted-ZrO_2 film are extensively investigated for nonvolatile memory applications. Reversible resistance-switching behavior from a high resistance to low resistance state can be traced by dc voltage and pulse voltage. After more than 200 dc switching cycles, the resistance ratio between the high and low resistance states is more than 180 times under 0.7 V readout bias. In the voltage pulse test, the "write" and "erase" speeds can be as fast as 50 and 100 ns, respectively. No data loss is observed for more than 10^6 s. The formation and rupture of conducting filamentary paths related to the implanted Au ions are suggested to be responsible for the resistive switching phenomenon. The dependence of resistance on temperature indicates that the variable-range hopping conduction mechanism is dominated in the low-resistance state, while the current characteristics are governed by the trap-controlled space limited conduction mechanism in the high-resistance state. © *2008 American Institute of Physics*. [DOI: 10.1063/1.3033561]

I. INTRODUCTION

Various new memory devices, such as phase random access memory (RAM),[1] magnetic random access memory,[2] nanocrystal floating gate memory,[3] and resistance RAM (RRAM),[4–16] have been proposed for future nonvolatile memory applications. Among all these candidates, RRAM has attracted extensive attention owing to its high density, low power, fast speed, and long retention.[4] The RRAM device has bistable resistive states, that is, both a high-resistance state (HRS) and low-resistance state (LRS). In external electrical spurring, reproducible bistable resistive switching behaviors were observed in various kinds of materials, such as ferromagnetic material,[5] organic material,[6] doped perovskite,[7] and binary transition metal oxides.[4,8–15] Among all these materials, binary transition metal oxides are preferred because of their simple structure, easy fabrication process, and compatibility with complementary metal-oxide semiconductor technology.[4] Up to now, various models have been proposed to explain resistive switching, such as the formation and rupture of the metallic filament,[7–13] Schottky barriers with interface states,[16] and trap charging and discharging.[14,15] With the use of any switching mechanism, the defects and impurities in the transition metal oxide will still play a critical role in resistive switching. Unfortunately, natural defects (such as dislocation, grain boundary, and vacancy) in transition metal oxide films are not uniformly distributed, resulting in difficulty to exactly control them, and thus lead to unstable resistive switching performances.[14] In the previous study,[14,15] the introduced external traps in ZrO_2 films could significantly improve performance, such as device yield and on/off ratio, because of more uniform and homogeneous trap concentrations. Ion implantation is a feasible way for introducing impurities and controlling their uniformity. However, to date, there is still no detailed and comprehensive research on memory characteristics of switching mechanisms.

In this study, ion implantation technique was used to fabricate the Au/Cr/Au-implanted-ZrO_2/n^+-Si sandwiched structure. The switching characteristics of the devices, including switching speed, endurance, and retention at room and high temperatures, were studied systematically. The physical origin of this switching phenomenon was also studied by temperature-dependent transport measurement.

II. EXPERIMENT

Resistive switching memory devices were fabricated on n^+ silicon wafer (3.5×10^{-3} Ω cm) after chemical cleaning. The device fabrication process was depicted as follows. First, a 70 nm ZrO_2 film was deposited through electron beam evaporation at a deposition rate of 1 Å/s, under a base pressure of 2.6×10^{-6} Torr, and followed by annealing at 800 °C for 120 s in N_2 ambient (2.5 l/min). Then, Au ions were implanted into the ZrO_2 film with 1×10^{11} cm^{-2} dose and 50 keV energies. To activate Au ions, the Au-implanted-ZrO_2 film was annealed at 400 °C for 5 s in N_2 ambient (2.5 l/min). Finally, the top electrodes of 10 nm thick Cr and 50 nm thick Au were evaporated by electron beam evaporation at a base pressure of 2.6×10^{-6} Torr. All the top electrodes were defined as squares (area from 100×100 to 1000×1000 μm^2) after the lift-off process. As comparison to confirm the effects of Au ions, a control sample without doping ZrO_2 was simultaneously fabricated. The Au-implanted-ZrO_2 film was characterized by x-ray dif-

[a)]Author to whom correspondence should be addressed. Electronic mail: liuming@ime.ac.cn. Tel.: 86-10-82995578. FAX: 86-10-82995583.

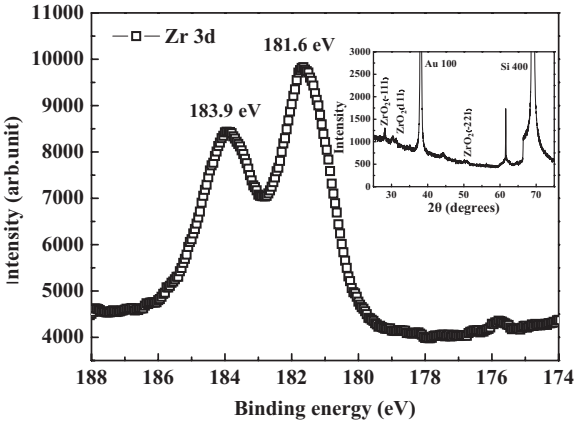

FIG. 1. The XPS spectra of Au-implanted-ZrO_2 film showing Zr^{4+} $3d_{5/2}$ (181.6 eV) and $d_{3/2}$ (183.9 eV) peaks. The inset figure is the 2θ scan XRD spectrum measured for Au/Cr/Au-implanted-ZrO_2/n^+-Si structure.

fraction (XRD) and x-ray photoelectron spectroscopy (XPS). The dc current-voltage (*I-V*) characteristics of the fabricated devices were measured using a Keithley 4200 semiconductor characterization system. Variation temperature measurement was performed in the vacuum chamber with the Lakeshore TTP4 probe station. The pulse test was performed with an Agilent 81110A pulse pattern generator and the Tektronix DPO 7104 oscilloscope. During electrical measurements, the positive bias was defined by the current flowing from the top electrode to the bottom electrode, and the opposite current flowing was defined as the negative bias.

III. RESULTS AND DISCUSSION

The XPS was shown in Fig. 1. The peaks of Zr $3d_{5/2}$ and Zr $3d_{3/2}$ at 181.6 and 183.9 eV (Ref. 12) showed that the zirconium was fully oxidized and existed as Zr^{4+} in the Au-implanted-ZrO_2 film. Given in the inset of Fig. 1 was the XRD pattern of the Au-implanted-ZrO_2 film; the (−111), (111), and (221) planes of ZrO_2 were clearly observed, indicating that the Au-implanted-ZrO_2 film exhibited high crystalline state after annealing at 800 °C.

Figures 2(a) and 2(b) showed the typical *I-V* characteristics of the Au/Cr/Au-implanted-ZrO_2/n^+-Si (denoted as the Au-implanted sample) device in semilogarithmic and logarithmic scales, respectively. Unlike most of the undoped transition-metal-oxide-based memory devices,[8–12] the Au-implanted sample did not need electroforming to develop resistance switching. In the case of the typical Au-implanted device, the original state was "on" and the initial resistance was about several decade kΩ at 0.7 V read voltage. When positive sweeping voltage ($0 \rightarrow 4$ V) was applied to the top electrode, a sudden drop in current appeared at reset voltage (V_{reset}), and the device switched from the LRS to the HRS, as shown in Fig. 2(a); this is defined as the "reset" process. Then, by sweeping the applied positive voltage ($0 \rightarrow 10$ V) with a current compliance of 10 mA, an abrupt increase in current appeared at set voltage (V_{set}), and the device switched from the HRS to the LRS; this is defined as the "set" process. The reset process can be achieved through applied negative voltage (data are not shown). This voltage-induced resistive switching can be traced hundreds of times.

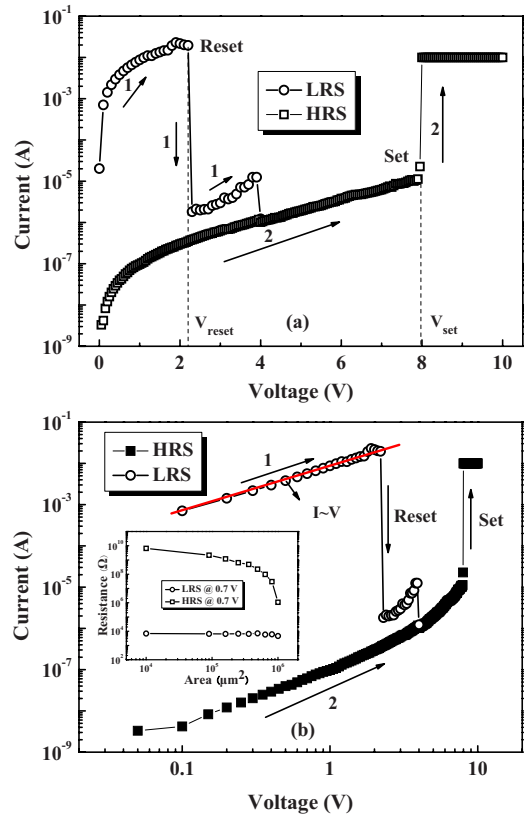

FIG. 2. (Color online) The typical *I-V* characteristics of the Au-implanted sample in (a) semilogarithmic scale and (b) double-logarithmic scale. The arrows indicate the sweeping directions. The slope of the fit line (red) is 1. The inset figure in (b) shows the resistance of Au-implanted sample dependence on cell area for both the on-state and off-state.

Under 0.7 V read voltage, the typical resistances of LRS and HRS were $\sim 10^3$ and $\sim 10^7$ Ω, respectively. Furthermore, almost every tested device showed the same reproducible switching behavior, and the device yield was nearly 100%. Compared with the Au-implanted sample, the initial resistance of the unimplanted sample was approximately $\sim 10^9$ Ω at 0.7 V. In the test involving more than 30 cells, different resistive switching phenomena in the unimplanted sample were observed. About 10% of the test cells showed unipolar switching phenomenon after the electroforming process (forming voltage was more than 10 V), as shown in Fig. 3(a). More than 40% of the test cells showed bipolar switching phenomenon under ±4 V switching voltage, which is similar to our previous work,[15] as shown in Fig. 3(b). The remains of the test cells showed unstable and noisy switching phenomena. Comparing the different resistive switching characteristics of both samples, it can be concluded that doping Au impurity in ZrO_2 films could significantly improve device-to-device performance and device yield because of the more uniform and homogeneous trap concentrations.

Conceivable mechanisms for resistive switching in RRAM often consist of interface or bulk effect based on where the switching originated. In the process of fabricating Au/Cr/Au-implanted-ZrO_2/n^+-Si and Au/Cr/ZrO_2/n^+-Si devices, the SiO_2 interfacial layer grew between Si and ZrO_2 after the process of annealing under the temperature of 800 °C. As characterized by scanning electron microscopy

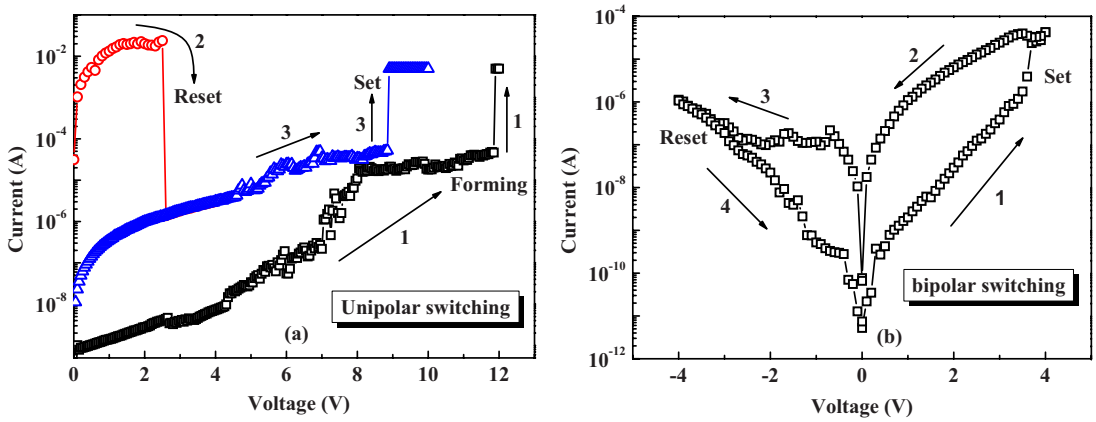

FIG. 3. (Color online) (a) The unipolar and (b) bipolar *I-V* characteristics of the unimplanted sample in the semilogarithmic scale, respectively. The arrows indicate the sweeping directions.

(data are not shown), the interfacial layer was about 5 nm. Based on experimental observations, it seemed that the resistive switching process has little relation to the interface effect. On one hand, typical resistive switching based on interface effects show bipolar characteristics,[16] whereas the resistive switching behaviors of the devices in our study showed no reliance on bias polarity. One the other hand, devices based on the Au-implanted and unimplanted films exhibited different switching performances, although they have similar interfaces. Therefore, it is suggested that bulk effects dominate the resistive switching behaviors of the devices.

According to our experimental results, the resistive switching behavior of the Au-implanted sample can be explained by the filament conductive mechanism. As shown in Fig. 2(b), it could be seen that the *I-V* characteristic in the on-state follows a linear Ohmic conduction (slope is close to 1). This is probably due to the formation of conducting filaments throughout the insulating film.[8–12] In order to confirm our proposition, the relationship between resistance and the device area was studied. As shown in the inset of Fig. 2(b), the resistance of the off-state increases with a reduced cell area, it can be seen that the resistance of on-state is insensitive to the cell sizes, indicating that the on current flows through localized conducting filamentary paths in the insulator, which confirmed that the filament transmission mechanism is the on-state. The area-dependent resistance suggests that the Au-implanted-ZrO_2 film can have a sufficient sensing margin when the device is scaled down.

Because the Au-implanted sample exhibited initial low resistance while the fresh unimplanted sample showed initial high resistance, it is believed that preformed filamentary conductive paths existed in the Au-implanted devices. Hence, it is suggested that the intentionally introduced Au impurities play an important role in forming conducting filamentary paths. To further study the conduction mechanism, electrical measurements in the temperature ranging from 100 to 420 K were carried out, as shown in Fig. 4. As seen in Fig. 4(a), the on-state's current increased with the rise in temperature, indicating that the filamentary path is not a metallic filament. As seen from the inset of Fig. 4(a), the best fit to the experimental data was obtained, assuming a dependence $\ln I \propto T^{-1/4}$, ranging from 200 to 400 K, following Motts's law of variable-range hopping (VRH).[17] It is suggested that Au ions might perform as localized hopping centers in the ZrO_2 lattice, giving rise to the observed conductivity in the on-state.

When the temperature increased from 100 to 420 K, the current of the device at off-state increased exponentially from 1.5×10^{-9} to 5.7×10^{-8} A [Fig. 4(b)], which is a typical semiconductor temperature characteristic. The conduction mechanism in the off-state can be explained by trap-controlled space charge limited conduction (SCLC).[18] Shown in Fig. 5 were the *I-V* characteristics under the off-state plotted on the double-logarithmic scale. The current is clearly divided into three parts: (i) the linear Ohmic behavior at the low voltage region (as shown in the bottom inset in Fig. 5), (ii) the square dependence on voltage when voltage is larger than 1 V (as shown in the upper inset in Fig. 5), and (iii) the steep increase in the higher voltage region. The off-state's current characteristic is in agreement with the trap-controlled SCLC.

According to the above analysis, the resistive switching phenomenon observed in the devices can be explained by the formation and annihilation of conducting filamentary paths that consist of Au ions. In the reset process, few conducting filamentary paths mainly conduct the large current; heating effect around these conducting filamentary paths during the

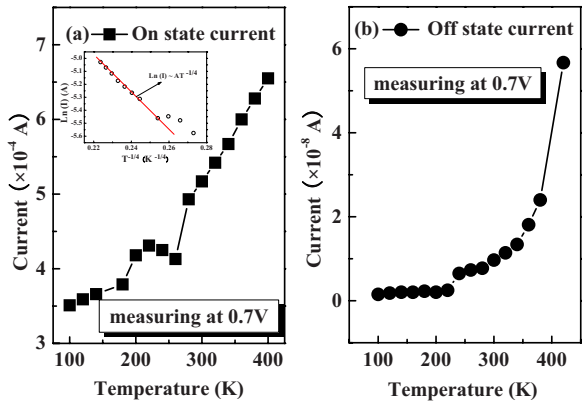

FIG. 4. (Color online) Temperature dependence of current in the (a) on-state and (b) off-state. The inset figure in (a) is fit with the VRH mechanism in the on-state.

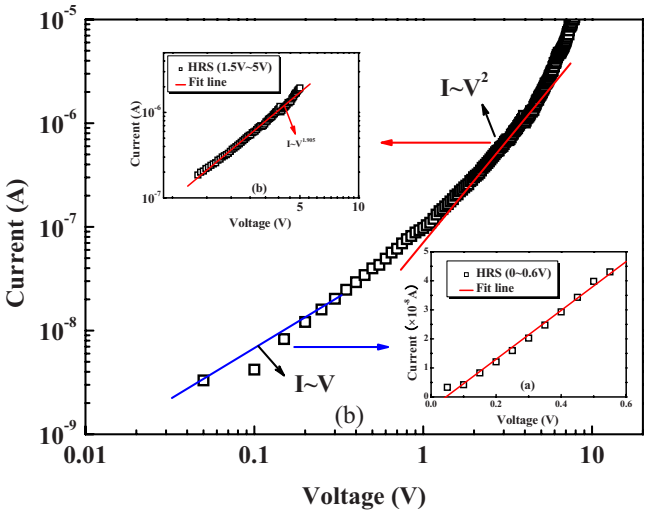

FIG. 5. (Color online) Replots of the off-state current in log-log scale. The upper inset shows that the *I-V* characteristics in high voltage range from 1.5 to 5 V and the fit line slope is 1.905. The bottom inset is the *I-V* characteristics in low voltage range from 0 to 0.6 V and the fit line slope is 1.

process of measurement is unavoidable, which causes the rise in the local area temperature around these filaments.[19] The Au ions are easy to disperse under high temperature, leading to localized rupture in these filaments. In this case, hopping distance (the length that electrons hop from one Au site to another) caused the current to reduce steeply, resulting in the device switch from LRS to HRS. It is known that extended defects, such as grain boundaries and dislocations, provide easy diffusion paths for oxygen or metal ions in metallic oxides.[20,21] In the set process, Au ions are easy to move and rearrange around the ZrO_2 grain boundaries under the high electric field, forming few tiny local conducting paths. When the voltage is increased to V_{set}, the tiny local conducting paths gather to form stronger conducting filaments. This is similar to the mechanism proposed by Choi *et al.*[9] to explain the formation of conducting filaments in TiO_2. Simultaneously, electrons hop in these paths through the

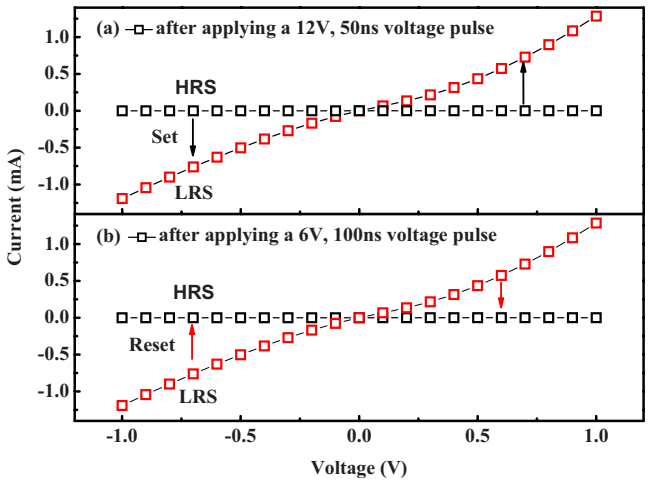

FIG. 6. (Color online) The resistive switching speed of the Au/Cr/Au-implanted-ZrO_2/n^+-Si structure under voltage pulse mode. (a) The speed of the set process (HRS→LRS) and (b) the speed of the reset process (LRS→HRS).

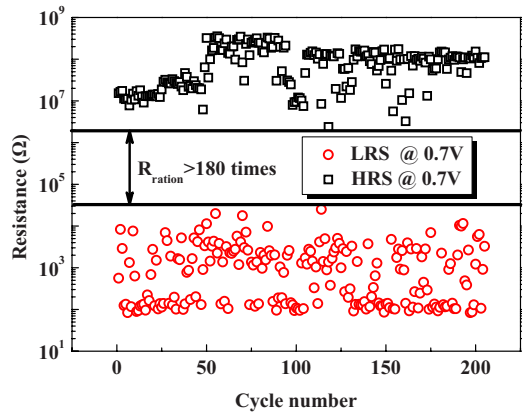

FIG. 7. (Color online) Resistance of Au/Cr/Au-implanted-ZrO_2/n^+-Si device in the on-state and off-state in 200 cycles with more than 180 times sensing margin under 0.7 V readout voltages.

ZrO_2 film, causing the current to increase dramatically. In this case, the device switches from HRS to LRS.

To evaluate the potential of this Au-implanted-ZrO_2-based memory for application in nonvolatile memory devices, switching speed, endurance, and retention tests were conducted. The resistive switching speed of the Au-implanted sample was investigated through a voltage pulse test, as shown in Fig. 6. In Fig. 6(a), before and after applying 12 V, 50 ns set voltage pulse, the *I-V* curve changes, showing that the device switched from HRS to LRS. On the other hand, the reset process can be done by applying 6 V at 100 ns voltage pulse, through which the device can switch back to HRS, as shown in Fig. 6(b).

Figure 7 showed the resistance of an Au-implanted film in the HRS and LRS versus the number of switching cycles at 0.7 V reading voltage. As shown, the dispersions of the resistance in the LRS and HRS were around 1×10^2–3×10^4 and 2×10^6–5×10^8 Ω, respectively. Though the resistances in both states are distributed widely, the margin of ratio between both states is more than 180 times. This is enough to be distinguished by a peripheral circuit. Figure 8 showed the retention performance tests of both LRS and HRS for the Au-implanted-ZrO_2 sample under 0.7 V reading voltage at room temperature (RT) and 85 °C, respectively. The resistances in the LRS and HRS were mostly unchanged for more than 10^6 s under RT, guaranteeing that both states

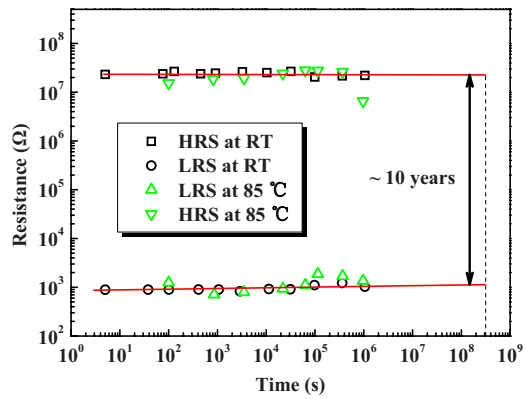

FIG. 8. (Color online) The retention characteristics of both resistance states at RT and 85 °C, respectively.

can be kept that way for more than 10 years by using the extrapolation method. Although the HRS resistance is reduced by about 50% for 10^6 s at 85 °C, the resistance ratio of the Au-implanted sample remained more than three orders of magnitude. After these retention tests, the device still shows reproducible switching behavior without obvious degradation. Fast speed, good endurance, and excellent retention characteristics of the Au-implanted-ZrO_2 film imply its promising potential for nonvolatile memory application.

IV. CONCLUSION

The Au/Cr/Au-implanted-ZrO_2/n^+-Si structure was fabricated and investigated for nonvolatile memory applications. It was found that the Au-implanted-ZrO_2 film exhibited stable and reproducible resistive switching behaviors. The results of the experiment showed that the dominant conduction mechanisms in the on-state and off-state were the VRH and trap-controlled SCLC, respectively. Considering that the Au/Cr/Au-implanted-ZrO_2/n^+-Si device shows high device yield, good endurance, fast speed, and long retention characteristics, the Au-implanted-ZrO_2-based memory has great potential for application in future nonvolatile resistive switching memory devices.

ACKNOWLEDGMENTS

This work was supported by the Hi-Tech Research and Development Program of China (863 Program) under Grant No. 2008AA031403, the National Basic Research Program of China (973 Program) under Grant No. 2006CB302706, and the National Natural Science Foundation of China under Grant Nos. 60825403, 90607022, and 60506005.

[1]S. Lai, Tech. Dig. - Int. Electron Devices Meet. **2003**, 255.
[2]D. C. Worledge and D. W. Abraham, Appl. Phys. Lett. **82**, 4522 (2003).
[3]S. Tiwari, F. Rana, H. Hanafi, A. Hartstein, E. F. Crabbe´, and K. Chan, Appl. Phys. Lett. **68**, 1377 (1996).
[4]I. G. Baek, M. S. Lee, S. Seo, M. J. Lee, D. H. Seo, D. S. Suh, J. C. Park, S. O. Park, H. S. Kim, I. K. Yoo, U-I. Chung, and I. T. Moon, Tech. Dig. - Int. Electron Devices Meet. **2004**, 587.
[5]S. Q. Liu, N. J. Wu, and A. Ignatiev, Appl. Phys. Lett. **76**, 2749 (2000).
[6]L. Ma, S. Pyo, J. Ouyang, Q. Xu, and Y. Yang, Appl. Phys. Lett. **82**, 1419 (2003).
[7]C. C. Lin, B. C. Tu, C. C. Lin, C. H. Lin, and T. Y. Tseng, IEEE Electron Device Lett. **27**, 725 (2006).
[8]S. Seo, M. J. Lee, D. H. Seo, E. J. Jeoung, D.-S. Suh, Y. S. Joung, I. K. Yoo, I. R. Hwang, S. H. Kim, I. S. Byun, J.-S. Kim, J. S. Choi, and B. H. Park, Appl. Phys. Lett. **85**, 5655 (2004).
[9]B. J. Choi, D. S. Jeong, S. K. Kim, S. Choi, J. H. Oh, C. Rohde, H. J. Kim, C. S. Hwang, K. Szot, R. Waser, B. Reichenberg, and S. Tiedke, J. Appl. Phys. **98**, 033715 (2005).
[10]D. Lee, D.-J. Seong, H. J. Choi, I. Jo, R. Dong, W. Xiang, S. Oh, M. Pyun, S.-O Seo, S. Heo, M. Jo, D.-K. Hwang, H. K. Park, M. Chang, M. Hasan, and H. Hwang, Tech. Dig. - Int. Electron Devices Meet. **2006**, 346733.
[11]G. Dearnaley, A. M. Stoneham, and D. V. Morgan, Rep. Prog. Phys. **33**, 1129 (1970).
[12]X. Wu, P. Zhou, J. Li, L. Y. Chen, H. B. Lv, Y. Y. Lin, and T. A. Tang, Appl. Phys. Lett. **90**, 183507 (2007).
[13]K. Jung, J. Choi, Y. Kim, H. Im, S. Seo, R. Jung, D. C. Kim, J.-S. Kim, B. H. Park, and J. P. Hong, J. Appl. Phys. **103**, 034504 (2008).
[14]W. Guan, S. Long, R. Jia, and M. Liu, Appl. Phys. Lett. **91**, 062111 (2007).
[15]Q. Liu, W. Guan, S. Long, R. Jia, M. Liu, and J. Chen, Appl. Phys. Lett. **92**, 012117 (2008).
[16]A. Sawa, T. Fujii, M. Kawasaki, and Y. Tokura, Appl. Phys. Lett. **85**, 4073 (2004).
[17]N. F. Mott, *Electronic Processes in Non-Crystalline Materials* (Clarendon, Oxford, 1979).
[18]M. A. Lampert and P. Mark, *Current Injection in Solids* (Academic, New York, 1970).
[19]Y. Sato, K. Kinoshita, M. Aoki, and Y. Sugiyama, Appl. Phys. Lett. **90**, 033503 (2007).
[20]K. Szot, W. Speier, R. Carius, U. Zastrow, and W. Beyer, Phys. Rev. Lett. **88**, 075508 (2002).
[21]G.-S. Park, X.-S. Li, D.-C. Kim, R.-J. Jung, M.-J. Lee, and S. Seo, Appl. Phys. Lett. **91**, 222103 (2007).